STUDY OF CR-39 AND MAKROFOL EFFICIENCY FOR RADON MEASUREMENTS

J.M. Stajic, B. Milenkovic and D. Nikezic

University of Kragujevac, Faculty of Science, Kragujevac, Serbia

Abstract

This paper presents experimental and theoretical determination of CR-39 and Makrofol calibration coefficients in diffusion chambers for radon measurements. Experimental calibration was performed by irradiation of detectors in calibration chamber where radon concentration was controlled with RAD7 device. Calculations were performed by the previously developed software for CR-39 detector. In addition the software was modified to enable calculation for Makrofol by implementing V function and other relevant data for this kind of detector.

A good agreement was found between experimental and theoretical approaches. The comparison enabled selecting V function for CR-39 that gave the best agreement with the experimental results.

Optimisation of chamber and detector dimensions was theoretically performed for different etching times. The dependence of calibration coefficient on ^{218}Po deposition fraction was also analysed.

Keywords: CR-39; Makrofol; Radon; Calibration coefficient; V function

Introduction

Solid state nuclear track detectors (SSNTD) are commonly used for radon measurements. Among them, the most often used are CR-39, LR115 and Makrofol. Detectors are used as a bare or in a cup closed with filter paper which is called "diffusion chamber". Various designs and dimensions of diffusion chambers were described in literature and used in practice. Some newer design were described by Calamosca et al., 2003; Csige and Csegzi, 2001; Nikolaev and Ilic, 1999; Nikezic and Yu, 2004; Sciocchetti et al., 2003; Torabi Nabil et al., 2012 etc. The output result of detector application (bare as well as closed in a cup) was track density per unit irradiation time. A detector in a diffusion chamber is pure radon measuring device (if the filter is enough thick to stop thoron diffusion into the chamber), while bare detectors can register all alpha emitters present in air: radon, thoron and their progeny.

To obtain the absolute value of average radon concentration during the irradiation, it is necessary to convert track density per irradiation time to radon concentration, by using calibration coefficient, *k*. Determination of *k* can be performed experimentally (Antovic et al., 2007; Garawi, 1996; Ismail and Jaafar, 2011) by exposing of detector to the known concentration under controlled laboratory conditions. Another approach is to calculate *k* by analytical or Monte Carlo methods (Eappen et al., 2008; Palacios et al., 2008; Patiris et al., 2012; Sima, 2001).

In this work, both methods, experiment and calculation, were applied in order to determine CC for CR-39 and Makrofol detectors placed in various diffusion chambers. CC for CR-39 was calculated by using different V functions found in literature and obtained results

were compared with calibration experiment. Optimal chamber and detector dimensions were theoretically determined for different etching times. Dimensions that correspond to minimal dependence of calibration coefficient on ^{218}Po deposition fraction were also reported.

Materials and methods

Calibration Experiment

The calibration experiment has been performed in Plexiglas chamber (of 30 L in volume) connected to RAD7 device (Durridge, Massachusetts, USA). A sample of uranium ore has been used as a source of radon in the chamber. Figure 1 presents the build up of radon concentration measured with RAD7. Four Makrofol (Iupilon®, with the thickness of 300 μm) and four CR-39 (TASTRAK®, 1 mm thick) detectors were placed in different semi-conical plastic cups with dimensions given in Table 1. Open ends of the cups were covered with filter paper in order to prevent radon progeny and aerosols from entering the detection volume. The detectors were exposed for 9 days.

Table 1. Dimensions of cups (R_1 – lower radius; R_2 – upper radius; H – height) and detectors (radius R_D) used in the experiment

Cup dimensions				Detector radius R_D [cm]	
No	**R_1[cm]**	**R_2[cm]**	**H[cm]**	**Makrofol**	**CR–39**
1	2.6	3.3	10	2.5	1.13
2	2.4	3.5	8.2	1.13	1.13
3	2.1	3	9.4	1.13	1.13
4	2.7	3.2	4.7	2.5	1.13

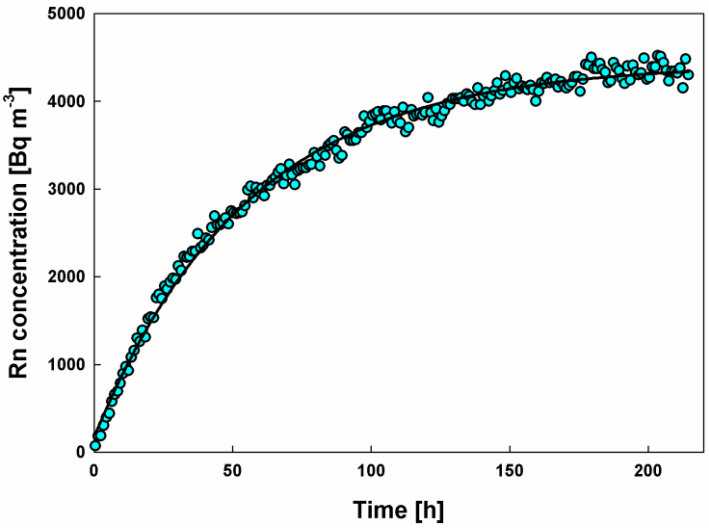

Figure 1. The build up of radon concentration inside the chamber. Measured with RAD7 device

After the exposure, CR-39 detectors were chemically etched in 6.25 N NaOH solution at 70^{0}C for 5 h. Makrofol detectors were etched for 2 h using PEW solution (15 g KOH + 45 g H_2O + 40 g ethyl alcohol) at the same temperature. The etched detectors were rinsed with distilled water in order to stop further etching. The tracks were counted manually using optical

microscope with 1000× magnification. Background track density was determined by observing unexposed detectors etched under the same conditions. Although some authors have reported the ability of polycarbonates to absorb certain amounts of radon in its volume (More and Hubbard, 1997; Pressyanov et al., 2000; 2003; 2004), a correction for radon absorption is not considered in this study. This effect is probably not too significant as the calibration factor due to radon absorption in Makrofol reported elsewhere (Pressyanov, 2009) is well lower than those for diffusion chambers, considered in the present study.

Calibration coefficient was obtained using the equation:

$$k = \frac{\rho}{\bar{C} \cdot \Delta t} \tag{1}$$

where ρ is the track density, Δt is the exposure time and $\bar{C}$ is the average radon concentration calculated from the equation (Stajic et al., 2015):

$$\bar{C} = \frac{\int_0^{\Delta t} C(t)dt}{\Delta t} = \alpha + \frac{\beta}{\gamma \cdot \Delta t} \cdot (1 - e^{-\gamma \cdot \Delta t}) \tag{2}$$

Parameters α, β and γ were obtained by fitting the experimental data presented in Figure 1. Accordingly, the mean radon concentration in the chamber was estimated to be 3350 Bq m^{-3} (the uncertainty of the estimate was calculated to be less than 8%, considering standard error of the mean and RAD7 calibration uncertainty).

Calibration coefficient is given in SI system in units (track/m^2)/(Bq·s/m^3) = m. In literature it is also given in (track/cm^2)/(Bq·h/m^3) or in (track/cm^2)/(Bq·d/m^3).

Bulk etch rates corresponding to the current etching conditions were estimated by gravimetrical methods. Masses of Makrofol and CR-39 detectors were measured before and after the etching. An analytical balance with the precision of 0.1 mg was used for these measurements. The values of (15 ± 1) μm h^{-1} and (1.06 ± 0.11) μm h^{-1} were obtained for Makrofol and CR-39, respectively. These values have been used for theoretical calculations.

Determination of calibration coefficient by Monte Carlo calculation

Previously developed Fortran90 computer program named CR39_Sensitivity (Nikezic et al., 2014) was used for theoretical calculation of calibration coefficient for CR-39 detector in a conical or cylindrical chamber. The program calculates the partial calibration coefficients for alpha particles produced by the decays of ^{222}Rn, ^{218}Po and ^{214}Po (it can also be used for thoron and its progeny). Three geometrically different irradiation conditions were considered in this software; (i) alphas emitted in volume of the cup, (ii) alphas emitted by progeny deposited onto cup walls (including filter) and (iii) alphas emitted by progeny plated out on the detector itself. Partial calibration coefficients are different for all three exposure situations. Total calibration coefficient, k_{tot} is obtained as a sum of partial calibration coefficients according to the equation:

$$k_{tot} = k_0 + f_1 k_{1a} + f_4 k_{4a} + (1 - f_1) k_{1w} + (1 - f_4) k_{4w} + k_{1p} + k_{4p} \tag{3}$$

where f_1 and f_4 are fractions of ^{218}Po and ^{214}Po decayed in air of the cup, (volumetric fractions) respectively; k_0 is partial calibration coefficient for ^{222}Rn in cup volume (assuming that there is no deposition of ^{222}Rn); k_{1a} and k_{4a} are calibration coefficients for ^{218}Po and ^{214}Po in cup volume, respectively; k_{1w} and k_{4w} are calibration coefficients for ^{218}Po and ^{214}Po deposited on

the cup wall; k_{1p} and k_{4p} are calibration coefficients for ^{218}Po and ^{214}Po deposited on the detector (plate out) (Nikezic et al., 2014).

Partial calibration coefficients are calculated separately, and total calibration coefficient is obtained by the formula given above. The following V functions for CR-39 detector were implemented in the software:

(A) $V = 1 + (11.45e^{-0.339R'} + 4e^{-0.044R'})(1 - e^{-0.58R'})$ (Durrani and Bull,1987)

(B) $V = 1 + e^{-0.1\,R'+1} - e^{-R'+1.27} + e^{1.27} - e^{1}$ (Brun et al.,1999)

(C) $V = 1 + e^{-0.068\,R'+1.1784} - e^{-0.6513\,R'+1.1784}$ (Yu et al., 2005a)

(D) $V = 1 + e^{-0.06082\,R'+1.119} - e^{-0.8055\,R'+1.119}$ (Yu et al., 2005b)

(E) $V = 1 + \frac{390}{(R'+2)^{2.35}} \cdot \ln(R'+1) \cdot \left(1 - e^{-R'/5}\right) + \frac{R'}{80}$ (Hermsdorf, 2009)

where R' represents residual range of alpha particles in CR-39. A detailed description of the software was given by Nikezic et al. (2014).

The same software has been modified in order to calculate the calibration coefficient for Makrofol. V function for Makrofol was found in literature (Benton and Nix, 1969; Somogyi et al., 1976; Vancraeynest et al., 1997):

$$V = 1 + \alpha \cdot REL^{\beta} \tag{4}$$

where REL represents restricted energy loss (in MeV cm^2 mg^{-1}) assuming the threshold energy for secondary electrons ω_0 = 1 keV. The values of parameters α = 0.096 and β = 2.82 have been applied in calculation (Somogyi et al., 1976). For the particle energies below 2 MeV (0.5 MeV/nucleon), total rate of energy loss, dE/dx (taken from SRIM-2013 computer code) (Ziegler et al., 1985) was used as REL. For the energies above 2 MeV, REL was obtained by substracting the energy lost through close collisions from the total rate of energy loss (Benton and Nix, 1969),

$$REL = \left(\frac{dE}{dx}\right) - \left(\frac{dE}{dx}\right)_{\omega>\omega_0} \tag{5}$$

The term $\left(\frac{dE}{dx}\right)_{\omega>\omega_0}$ was calculated according to formulae given by Somogyi et al. (1976).
V function for Makrofol determined in above described manner as a function of residual range (R') is presented in Figure 2.

For the purposes of the calculation in abovementioned software, it is more convenient to use one equation rather than data in a table, and points in Figure 2 were fitted by the following function:

$$V(R') = \sum_{i=1}^{5} a_i R'^{b_i} e^{c_i R'} \tag{6}$$

where a_i, b_i and c_i are fitting parameters presented in Table 2.

Table 2. Parameters of the function *V(R')* for Makrofol obtained by fitting

	1	*2*	*3*	*4*	*5*
a	0.1317	0.5222	0.3903	0.4660	0.0684
b	1.9551	-0.0481	4.2384	0.0632	0.5890
c	-0.4055	0.0001	-1.4833	-0.0006	-0.0797

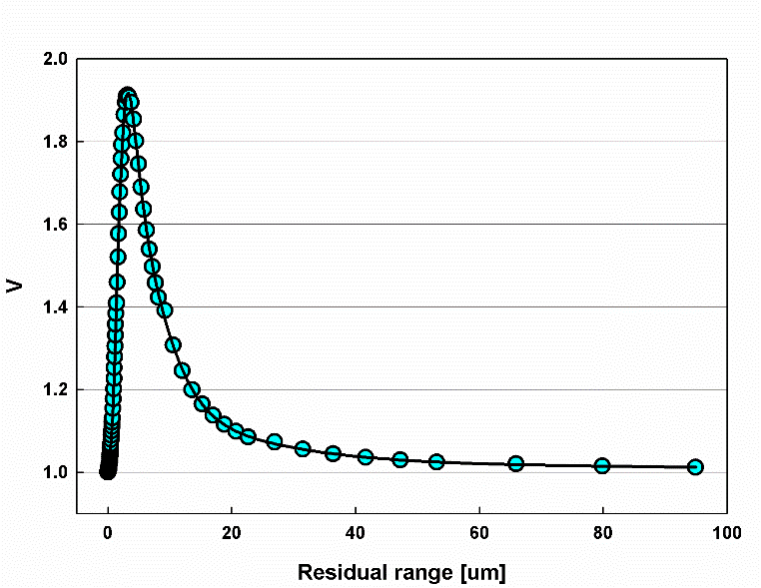

Figure 2. V function for Makrofol. Scattered dots are produced by Equation (4) and data from SRIM 2013. Solid line is fit with Eq. (6) and parameters given in Table 2.

Results and discussion

Figure 3 presents comparison of the experimental results with Monte Carlo calculation for CR-39 detectors placed in four different cups. Dash lines present the results of experimental calibration. The highest calibration coefficient was obtained for cup 1.

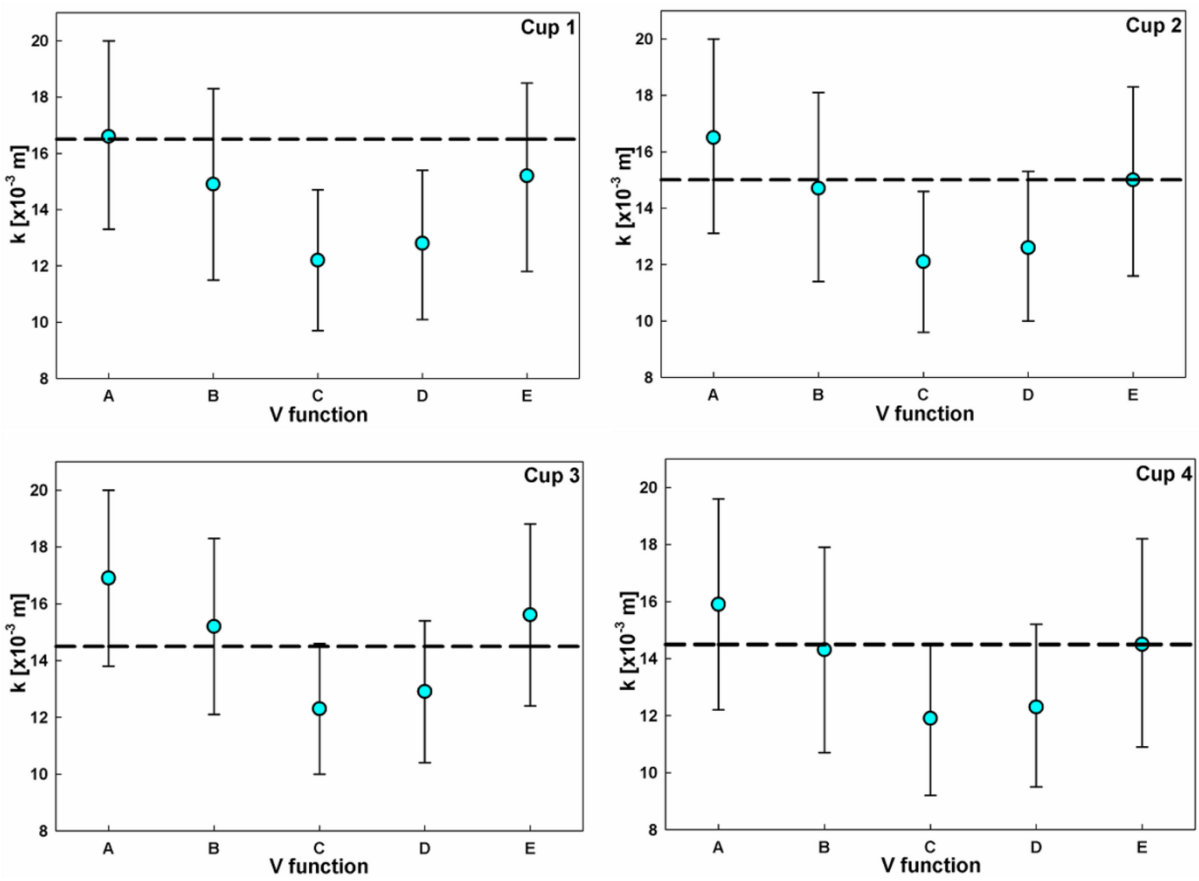

Figure 3. Calibration coefficients obtained from experiment (dash line) and software (dots with error bars) for CR-39 detectors and five different V functions (A-E)

The range of calibration coefficients presented by error bars were obtained by calculation for the values $f_1=1$ and $f_1=0$ (f_1 is the fraction of ^{218}Po that decays in the air, before the deposition). Previously mentioned five V functions have been applied. It can be seen from Figure 3 that the functions A, B and E gave the best agreement with the experiment. The intervals obtained using the function D included some of the experimental values while the function C underestimates experimental results in all cases. Similar conclusion was made by Nikezic et al. (2014) based on comparison with the experimental results reported by other authors (references are cited therein). The dimensions of cups and detectors, as well as, the etching conditions used in this work are different from those applied in the previous studies.

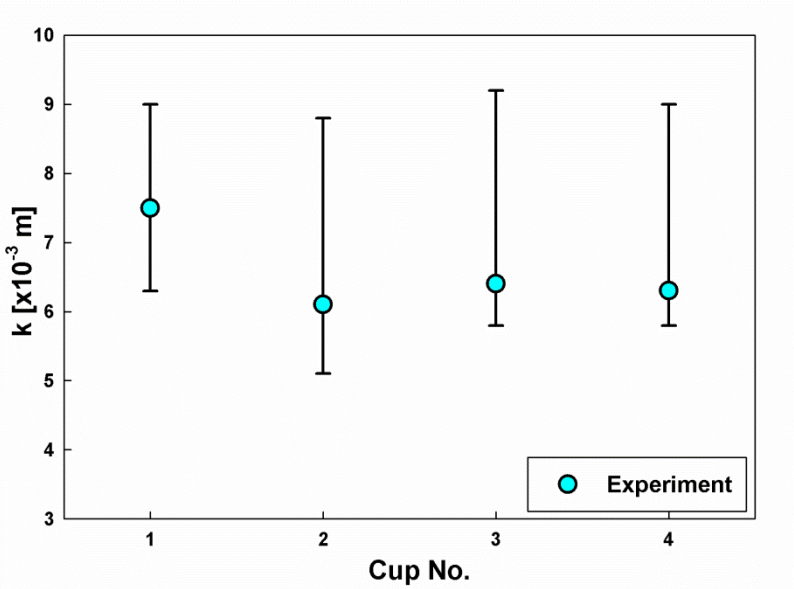

Figure 4. Calibration coefficients obtained from experiment (dots) and software (error bars) for Makrofol detector

Figure 4 presents the results of calibration of Makrofol detectors. All experimental values fell into the intervals of theoretically obtained results. It can be seen that the experimental results are either in the middle of the theoretical intervals, or even closer to the lower limits corresponding to the fraction f_1=0. It indicates that most of ^{218}Po atoms decay after the deposition. This result is in agreement with previous studies witch have suggested that volumetric fraction of ^{218}Po is probably less than 0.5 (Koo et al., 2002; Koo et al. 2003; McLaughlin and Fitzgerald, 1994).

The uncertainties of the experimental values were estimated to be up to 20% for both Makrofol and CR-39 calibration coefficients. The estimation was made taking into account the uncertainties of all parameters appearing in equation (1).

Software was also used to investigate the dependence of calibration coefficient on cup height. The height was varied with a step of 0.5 cm for fixed radii R_1 = 2.5 cm, R_2 = 2.5 cm and R_D = 2.5 cm. The results are presented in Figure 5. Calibration coefficient increases with enlarging of cup height and it reaches a nearly constant value at H ≈ 7 cm. This result is in accordance with the fact that the range of alpha particles emitted by ^{214}Po (7.69 MeV) in air is approximately 7 cm (SRIM 2013).

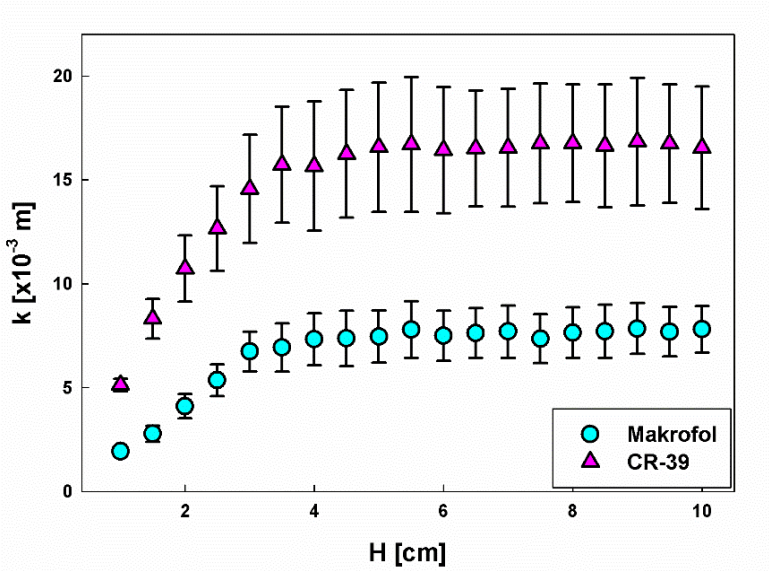

Figure 5. Calculated calibration coefficient as a function of cylindrical cup height. The dimensions R_1=2.5 cm, R_2=2.5 cm and R_D=2.5 cm were assumed.

It is important to mention that the upper limits of error bars on Figure 5 (for both, Makrofol and CR-39) correspond to f_1=1. Besides, it is obvious that the ranges of error bars increase with increasing of cup height. The dimensions of cups corresponding to the minimal ranges of error bars are the most optimal from the point of view of decreasing the uncertainty introduced in calibration coefficient due to the fraction f_1.

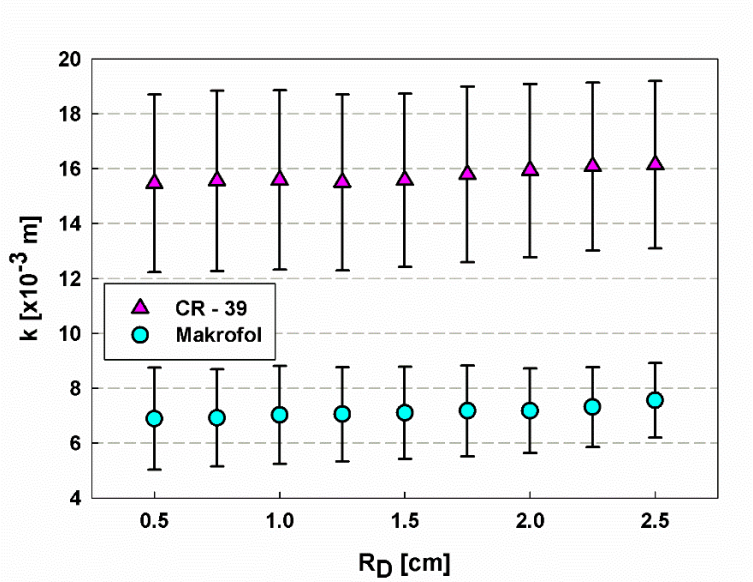

Figure 6. Calculated calibration coefficient as a function of detector radius. The dimensions R_1=2.5 cm, R_2=2.5 cm and H=5 cm were assumed

Figure 6 presents a slight increase of calibration coefficient associated with increasing of detector radius. As expected, such increase is mainly observable for f_1=0 (lower limits of error bars). This result indicates inhomogeneous distribution of alpha particle tracks on detector surface i.e. track density slightly increases with approaching the side walls of the cup. The cup dimensions were fixed at: R_1=2.5 cm, R_2=2.5 cm and H=5 cm.

Software was also used for determination of optimal chamber and detector dimensions that correspond to the highest calibration coefficient for different etching times (under the same etching conditions). The dimensions were varied with a step of 0.25 cm, within the following ranges: 1 cm $\leq H \leq$ 7 cm; 1 cm $\leq R_2 \leq$ 7 cm; 1 cm $\leq R_1 \leq R_2$ cm; 0.5 cm $\leq R_D \leq R_1$ cm. The results are presented in Table 3. The values of maximum calibration coefficient (k_{max}) given in the table was calculated assuming f_1=0.5.

Table 3. Dimensions of cups and detectors that correspond to the highest calibration coefficients (k_{max}) for different etching times (t_e)

CR-39					
t_e [h]	**k_{max} [$\times 10^{-2}$ m]**	**R_1 [cm]**	**R_2 [cm]**	**H [cm]**	**R_D [cm]**
5	2.69 ± 0.03	6.75	6.75	7.00	0.75
10	3.08 ± 0.07	6.75	6.75	7.00	0.50
15	3.27 ± 0.01	6.25	7.00	7.00	0.50
Makrofol					
t_e [h]	**k_{max} [$\times 10^{-3}$ m]**	**R_1 [cm]**	**R_2 [cm]**	**H [cm]**	**R_D [cm]**
0.5	3.58 ± 0.56	6.75	6.75	5.00	1.50
1	5.54 ± 0.86	6.75	6.75	4.00	5.25
2	9.37 ± 0.89	4.75	6.25	7.00	1.50

The range of *k* obtained for different values of ^{218}Po deposition fraction was also examined. Dimensions of cups and detectors that correspond to minimal dependence of *k* on f_1 were presented in Table 4.

Table 4. Dimensions of cups and detectors that correspond to minimal dependence of calibration coefficient on ^{218}Po deposition (f_1) for different etching times (t_e)

CR-39					
t_e[h]	**k [$\times 10^{-2}$ m]**	**R_1 [cm]**	**R_2 [cm]**	**H [cm]**	**R_D [cm]**
5	0.55 ± ng*	7.00	7.00	1.00	4.00
10	2.07 ± ng*	5.75	6.50	6.00	1.50
15	2.23 ± 0.03	3.75	7.00	5.00	0.50
Makrofol					
t_e[h]	**k [$\times 10^{-3}$ m]**	**R_1 [cm]**	**R_2 [cm]**	**H [cm]**	**R_D [cm]**
0.5	2.23 ± ng*	5.5	6.25	3.50	4.75
1	1.50 ± ng*	1.00	2.50	2.00	0.50
	2.67 ± ng*	4.75	5.50	2.50	1.25
2	1.86 ± 0.19	5.75	6.00	1.00	5.75

* the value is negligible

Conclusion

Calibration coefficients for radon measurements using CR-39 and Makrofol were calculated by experimental and theoretical methods. Previously developed software was adjusted for Makrofol calibration by applying appropriate V function for polycarbonates. Comparison of two approaches confirmed the applicability of the software for calculation of calibration factor for radon measurements.

Several V functions for CR-39, taken from literature, were compared, in order to select once that give the best agreement with experimental results. It has been found that functions A and E are in good agreement with experimental results.

The software was also used for determination of optimal chamber and detector dimensions for different etching times. Dimensions that correspond to minimal dependence of calibration coefficient on ^{218}Po deposition fraction were also reported.

By comparison of experimental data on Fig 3 (horizontal dotted line) and Fig 4 (scatter points) one can estimate that CR-39 detector is about two times more sensitive than Makrofol detector. This result is expectable because Makrofol has detection energy window in differ to CR-39.

In Fig 6, dependence of calibration coefficient on detector radius is presented. It could be seen that calibration coefficient weakly depends (almost constant) on detector radius, i.e., track density is almost constant along the detector. It is interesting that the same is true for both detectors.

Results given in Table 3 shows increasing of maximal calibration coefficient with the etching time. However, increment is much larger for the Makrofol than for CR-39.

Acknowledgement

The present work was supported by the Ministry of Education, Science and Technology Development of the Republic of Serbia, under the Project No. 171021.

References

Antovic, N., Vukotic P., Zekic, R., Svrkota, R., Ilic, R., 2007. Indoor radon concentrations in urban settlements on the Montenegrin Coast. Radiat. Meas. 42, 1573-1579.

Benton, E.V., Nix, W.D., 1969. The restricted energy loss criterion for registration of charged particles in plastics. Nucl. Instrum. Methods 67, 343-347.

Brun, C., Fromm, M., Jouffroy, M., Meyer, P., Groetz, J.E., Abel, F., Chambaudet, A., Dorschel, B., Hermsdorf, D., Bretschneider, R., Kadner, K., Kuhne, H., 1999. Intercomparative study of the detection characteristics of the CR-39 SSNTD for light ions: Present status of the Besancon-Dresden approaches. Radiat. Meas. 31, 89-98.

Calamosca, M., Penzo, S., Gualdrini, G., 2003. The features of the new radon gas CR-39 dosemeter developed at the ENEA Institute of Radioprotection. Radiat. Meas. 36, 221–224.

Csige, I., Csegzi, S., 2001. The Radamon radon detector and an example of application, Radiat. Meas. 34, 437–440.

Durrani, S.A., Bull, R.K., 1987. Solid State Nuclear Track Detection. Principles Methods and Applications, Pergamon Press.

Eappen, K. P., Sahoo, B. K., Ramachandran, T. V., Mayya, Y. S., 2008. Calibration factor for thoron estimation in cup dosimeter. Radiat. Meas. 43, S418-S421.

Garawi, M. S., 1996. Measurement of Radon Concentration in Private Houses in the Eastern Part of Al-Qaseem Province of Saudi Arabia. Radiat. Prot. Dosim. 63, 227–230.

Hermsdorf, D., 2009. Measurement and comparative evaluation of the sensitivity V for protons and hydrogen isotopes registration in PADC detectors of type CR-39. Radiat. Meas. 44, 806–812.

Ismail, A. H., Jaafar, M. S., 2011. Design and construct optimum dosimeter to detect airborne radon and thoron gas: Experimental study. Nucl. Instrum. Meth. Phys. Res. B 269, 437-439.

Koo, V.S.Y., Yip, C.W.Y., Ho, J.P.Y., Nikezic, D., Yu, K.N., 2002. Experimental study of track density distribution on LR115 detector and deposition fraction of ^{218}Po in diffusion chamber. Nucl. Instr. Meth. Phys. Res. A 491, 470–473.

Koo, V.S.Y., Yip, C.W.Y., Ho, J.P.Y., Nikezic, D., Yu, K.N., 2003. Deposition fractions of ^{218}Po in diffusion chambers. Appl. Radiat. Isot. 59, 49–52.

McLaughlin, J.P., Fitzgerald, B., 1994. Models for determining the response of passive alpha particle detectors to radon and its progeny in cylindrical detecting volumes. Radiat. Prot. Dosim. 56, 241–246.

Möre, H., Hubbard, L.M., 1997. ^{222}Rn Absorption in Plastic Holders for Alpha Track Detectors: A Source of Error. Radiat. Prot. Dosim. 74, 85-91.

Nikezic, D., Yu, K.N., 2004. Formation and growth of tracks in nuclear track materials. Mater. Sci. Eng. R 46, 51–123.

Nikezic, D., Yu, K.N., Stajic, J.M., 2014. Computer program for the sensitivity calculation of a CR-39 detector in a diffusion chamber for radon measurements. Rev. Sci. Instrum. 85, 022102.

Nikolaev, V.A., Ilic, R., 1999. Etched track radiometers in radon measurements: a review, Radiat. Meas. 30 1–13.

Palacios, D., Palacios, F., Sajo-Bohus, L., Barros, H., Greaves, E. D., 2008. LR-115 detector response to ^{222}Rn, ^{220}Rn and their progenies, exposed to hemispherical surfaces in free air, and design of a system to calculate their concentrations. Radiat. Meas. 43, S435-S439.

Patiris, D. L., Blekas, K., Ionnides, K. G., 2007. TRIAC II. A MatLab code for track measurements from SSNT detectors. Comput. Phys. Commun. 177, 329-338.

Pressyanov, D., Buysse, J., Poffijn, A., Meesen, G., Van Deynse A., 2000. Polycarbonates: a long-term highly sensitive radon monitor. Nucl. Instr. Meth. Phys. Res. A 447, 619-621.

Pressyanov, D., Buysse, J., Poffijn, A., Meesen, G., Van Deynse, A., 2003. The compact disk as radon detector – a laboratory study of the method. Health Phys. 84, 642-651.

Pressyanov, D., Buysse, J., Poffijn, A., Van Deynse A., Meesen, G., 2004. Integrated measurements of ^{222}Rn by absorption in Makrofol. Nucl. Instr. Meth. Phys. Res. A 516, 203-208.

Pressyanov, D., 2009. Modeling a 222Rn measurement technique based on absorption in polycarbonates and track-etch counting. Health Phys. 97, 604-612.

Sciocchetti, G. Cotellessa, G., Soldano, E., Pagliari, M., 2003. A new technique for measuring radon exposure at working places, Radiat. Meas. 36, 199–203.

Sima, O., 2001. Monte Carlo simulation of radon SSNT detectors. Radiat. Meas. 34, 181–186.

Somogyi, G., Grabisch, K., Scherzer, R., Enge, W., 1976. Revision of the concept of registration threshold in plastic track detectors. Nucl. Instrum. Methods 134, 129-141.

Stajic, J.M., Milenkovic, B., Nikezic, D., 2015. Radon concentrations in schools and kindergartens in Kragujevac city, Central Serbia. CLEAN – Soil, Air, Water 43, 1361-1365.

Torabi Nabil, F., Hosseini Pooya, S.M., Shamsaie Zafarghandi, M., Taheri, M., 2012. A diffusion chamber for passive separated measurements of radon/thoron concentration in dwellings. Nucl. Instr. Meth. Phys. Res. A 694, 331-334.

Vancraeynest, G., Franchoo, S., Huyse M., Moons, R., 1997. Optimisation and modelling of electrochemically etched polycarbonate track detectors. Nucl. Instr. Meth. Phys. Res. B 129, 65-72.

Yu, K.N., Ho, J.P.Y., Nikezic, D., Yip, C.W.Y., 2005a. Determination of the V function for CR-39 by atomic force microscope. In Recent advances in multidisciplinary applied physics. Elsevier, Amsterdam, p.29-34.

Yu, K.N., Ng, F.M.F., Nikezic, D., 2005b. Measuring depths of sub-micron tracks in a CR-39 detector from replicas using atomic force microscopy. Radiat. Meas. 40, 380-383.

Ziegler, J.F., Biersack, J.P., Littmark, U., 1985. The Stopping and Ranges of Ions in Solids, Pergamon Press, Oxford. SRIM 2013 (http://www.SRIM.org).